

Regularized Schrödinger Bridge: Alleviating Distortion and Exposure Bias in Solving Inverse Problems

Qing Yao¹, Lijian Gao¹, Qirong Mao¹, Ming Dong²

¹Jiangsu University

²Wayne State University

qyao@stmail.ujs.edu.cn, {ljgao, mao_qr}@ujs.edu.cn, mdong@wayne.edu

Abstract

Diffusion models serve as a powerful generative framework for solving inverse problems. However, they still face two key challenges: 1) the *distortion-perception tradeoff*, where improving perceptual quality often degrades reconstruction fidelity, and 2) the *exposure bias problem*, where the training-inference input mismatch leads to prediction error accumulation and reduced reconstruction quality. In this work, we propose the Regularized Schrödinger Bridge (RSB), an adaptation of Schrödinger Bridge tailored for inverse problems that addresses the above limitations. RSB employs a novel regularized training strategy that perturbs both the input states and targets, effectively mitigating exposure bias by exposing the model to simulated prediction errors and also alleviating distortion by well-designed interpolation via the posterior mean. Extensive experiments on two typical inverse problems for speech enhancement demonstrate that RSB outperforms state-of-the-art methods, significantly improving distortion metrics and effectively reducing exposure bias.

Introduction

Solving inverse problems is crucial in image and audio processing, finding extensive applications such as image restoration (Whang et al. 2021; Kawar et al. 2022) and speech enhancement (Richter et al. 2023; Lemercier et al. 2023). Typically, the goal is to recover the clean data from the degraded counterpart accurately. But due to its *ill-posed* nature (Richardson 1972), it is challenging to solve because there exist multiple solutions for a degraded observation. As a result, different categories of methods have been proposed, aiming to find different types of plausible solutions.

Traditional predictive methods try to produce a deterministic output by end-to-end supervised training of neural networks (Ongie et al. 2020; Whang et al. 2021). These methods strive to minimize distortion by directly modeling the deterministic mapping between clean and degraded signals, but suffer from the problem of “regression to the mean.” They often yield overly-smoothed outputs (Ongie et al. 2020), sacrificing perceptual quality. Another line of work, generative methods, focuses on enhancing perceptual realism by modeling the underlying distribution of clean data to produce more natural and realistic outputs. Recent advances in diffusion models (Ho, Jain, and Abbeel 2020; Song et al. 2021) have demonstrated remarkable generative

capabilities and have significantly advanced the state-of-the-art performance in solving inverse problems.

Despite great advancements, there are two critical challenges with diffusion models: **distortion-perception (DP) tradeoff** and **exposure bias problem**. First, the ill-posed nature of inverse problems manifests as the **DP trade-off** (Blau and Michaeli 2017; Freirich, Michaeli, and Meir 2021; Adrai et al. 2023; Zhou et al. 2025; Ohayon, Michaeli, and Elad 2025), which refers to the difficulty of simultaneously optimizing perceptual quality and reconstruction fidelity, as improving perceptual quality typically entails sacrificing distortion performance. In diffusion models, recent hybrid work (Whang et al. 2021; Lemercier et al. 2023) proposes a family of cascade methods combining predictive and generative models by starting the sampling from the minimal distortion estimate (i.e., the posterior mean) in the reverse diffusion process, leading to improvements in balancing the tradeoff (Whang et al. 2021). Second, **exposure bias problem** (Ning et al. 2023b; Li et al. 2023; Ren et al. 2024) further complicates matters. It arises from discrepancies between the training phase, where neural networks are trained on one-step ground-truth input, and the inference phase, where methods are limited by their reliance on the previously predicted samples as input. This mismatch leads to accumulated prediction errors during inference (Ning et al. 2023b), significantly degrading the overall quality of the generated output. Efforts to mitigate potential inference-time prediction errors during training and to improve the actual reconstruction quality are at an early stage (Ning et al. 2023b; Li et al. 2023).

Schrödinger bridge (SB) (Chen, Liu, and Theodorou 2022; Liu et al. 2023; Jukić et al. 2024), an extension of score-based diffusion models, has emerged as a promising generative framework for many tasks such as image generation and speech synthesis. SB leverages an optimal transport viewpoint to reach the target distribution in finite sampling steps and is able to deliver high perceptual realism while remaining computationally efficient. In this paper, we propose the **Regularized Schrödinger Bridge (RSB)**, an extension of SB-based diffusion models, for solving inverse problems. In RSB, we formulate a time-varying interpolation between two critical endpoints: the posterior mean (minimal distortion) and the ground-truth data (optimal perception). This interpolation serves as a perturbation to the training objec-

tive to guide the model to generate predictions aligned with the DP curve, the theoretical boundary representing the optimal tradeoff between distortion and perception, resulting in a better DP tradeoff. Additionally, RSB introduces a novel training regularization method that simulates the possible prediction errors during training, narrowing the training-inference mismatch and thus reducing exposure bias.

The major contributions of our work are summarized as follows:

- We propose RSB tailored for solving inverse problems, which introduces a novel DP regularization method in order to simultaneously alleviate exposure bias and reduce distortion.
- From a theoretical perspective, we introduce the posterior mean to the interpolation perturbation and use it to simulate prediction errors. Our regularized training with perturbation actively guides the model predictions towards the optimal DP tradeoff and exposes our model to simulated inference-time prediction errors, leading to more faithful and perceptually plausible results for ill-posed inverse problems.
- We validate the effectiveness of RSB on two typical audio inverse tasks for speech enhancement: speech denoising and dereverberation. Extensive experiments demonstrate that RSB outperforms state-of-the-art generative speech enhancement methods, significantly improving distortion metrics and effectively reducing exposure bias.

Related Work

Diffusion Models for Inverse Problems. Diffusion models have emerged as a powerful framework for solving inverse problems across vision and audio domains. Previous work involves conditioning denoising diffusion models (Saharia et al. 2021; Lu et al. 2022), which start from Gaussian noise, on degraded measurements during inference, or leverages stochastic differential equations (SDEs) to explicitly model the transport from the measurement distribution to the clean data distribution (Whang et al. 2021; Kawar et al. 2022). More recently, *bridge* model, such as Diffusion Bridges (Zhou et al. 2023), Brownian Bridges (Wang et al. 2024), have attracted significant attention. However, although advancements in diffusion models have achieved notable perceptual realism, challenges related to the DP tradeoff and exposure bias remain inadequately addressed.

Distortion–Perception Tradeoff. In inverse problems, multiple solutions exist for a given measurement, which is referred to as ill-posedness. This gives rise to the DP tradeoff (Blau and Michaeli 2017), which is fundamental for evaluating algorithms that address inverse problems. Specifically, these algorithms often balance between the *distortion*, which quantifies the average reconstruction error, and the *perception*, which quantifies the divergence between the two distributions. Because these objectives are antagonistic, improving one typically degrades the other (Blau and Michaeli 2017). Consequently, this tradeoff is generally formulated as minimizing distortion under a given level of perceptual quality. The optimal solutions under various perceptual quality

constraints collectively form the DP tradeoff curve, where the ideal optimal solution to the inverse problem is achieved when distortion is minimized under the best possible perceptual quality. To achieve this optimal solution, a common practice (Freirich, Michaeli, and Meir 2021) involves first obtaining the minimum-distortion estimate (e.g., the minimal Mean Squared Error (MSE) prediction) and then optimally transporting it to the target data distribution. Building on this idea, recent hybrid approaches consider employing a diffusion model to refine the details of the initial minimal MSE estimate (Whang et al. 2021; Lemercier et al. 2023). However, these methods still require multiple-step sampling, which may exacerbate the exposure bias issue.

Exposure Bias Problem. Exposure bias is a notable limitation of diffusion models that stems from discrepancies between training (conditioned on ground-truth data) and inference (conditioned on previously generated samples) (Ning et al. 2023b). Even slight prediction errors therefore accumulate over dozens or hundreds of timesteps, potentially pushing the trajectory progressively farther from the true data manifold (Ning et al. 2023b). In denoising diffusion models, existing strategies fall into two categories: training methods that simulate prediction errors, such as input perturbation (Ning et al. 2023b) and scheduled sampling (Ren et al. 2024), forcing the network to learn to recover from its own mistakes; and inference-time adjustments, such as output scaling (Ning et al. 2023a) or time-step shifting (Li et al. 2023), which realign the trajectory toward the data manifold without retraining. Notably, these approaches fundamentally rely on the Gaussian noise-to-data process in the denoising process, making them incompatible with bridge diffusion models that operate under fundamentally different data-to-data processes. However, more profound exploration of exposure bias within SB frameworks remains scarce, motivating the present study.

Speech Enhancement. Speech Enhancement (SE) is a typical acoustic inverse problem that aims to improve the quality and intelligibility of degraded speech, typically corrupted by noise and reverberation. Among diffusion-based SE methods, CDiffuSE (Lu et al. 2022) is a time-domain conditional diffusion model that starts from Gaussian noise and guides the reverse process with the noisy mixture to reconstruct the clean waveform. SGMSE+ (Richter et al. 2023) proposes a score-based diffusion model in the complex spectrogram domain, which introduces an SDE-based process to transport from noisy speech distribution to clean speech distribution. SGMSE+ can generate high-quality reconstructions using only 30 steps (Richter et al. 2023), but it still suffers from high distortion. A hybrid SE method StoRM (Lemercier et al. 2023) cascades a predictive model with a diffusion model to balance this DP tradeoff. Recently, Jukić et al. adapted the SB framework to SE, delivering improved perceptual realism while maintaining a moderate computational cost. However, the DP tradeoff and exposure bias of SB remain open issues. Our proposed RSB builds on the SB framework to address these two limitations, as empirically verified against the aforementioned baselines.

Regularized Schrödinger Bridge

This section presents RSB, an extension of SB tailored for inverse problems via Distortion-Perception (DP) regularization. We first define the specific formulation of SB in the context of inverse problems, and then examine the behavior of model predictions to further analyze the DP tradeoff and exposure bias issues in SB. Finally, we present DP regularization in detail.

Schrödinger Bridge for Inverse Problems

Let the clean data x be a realization of a random vector X with probability density function p_X . The degraded measurement y (e.g., noisy speech in SE) is a realization of a random vector Y . Given y , our objective is to draw an estimate \hat{x} from the posterior distribution $p_{\hat{X}|Y}(\cdot | y)$ such that \hat{x} faithfully reconstructs x .

The SB problem (Kantorovich 2006) is an entropy-regularized optimal transport problem between two distributions. In inverse problems, we formulate SB as a principled framework to find the optimal transport between the clean data distribution p_X and the measurement distribution p_Y . As the SB problem can be equivalently defined by a pair of forward-backward SDEs (Chen et al. 2023), let X_t be the intermediate state at $t \in [0, 1]$ with boundaries $X_0 = x \sim p_X$ and $X_1 = y \sim p_Y$, and SB can be expressed as,

$$\begin{aligned} dX_t &= [\mathbf{f} + g^2(t)\nabla \log \Psi_t]dt + g(t)d\mathbf{W}, \\ dX_t &= [\mathbf{f} - g^2(t)\nabla \log \hat{\Psi}_t]dt + g(t)d\bar{\mathbf{W}}, \end{aligned} \quad (1)$$

where \mathbf{f} and g denotes the drift and diffusion coefficient, respectively. \mathbf{W} and $\bar{\mathbf{W}}$ are Wiener processes. $\log \Psi_t$ and $\log \hat{\Psi}_t$ denote the time-varying energy functions.

Generally, solving SB is intractable, so we pursue closed-form solutions under Gaussian boundary conditions (Chen et al. 2023; Jukić et al. 2024). Given paired data (x, y) , the solution can be derived as,

$$\hat{\Psi}_t = \mathcal{N}(\alpha_t x, \alpha_t^2 \sigma_t^2 I), \Psi_t = \mathcal{N}(\bar{\alpha}_t y, \bar{\alpha}_t^2 \bar{\sigma}_t^2 I), \quad (2)$$

where $\alpha_t = e^{\int_0^t f(\tau)d\tau}$, $\sigma_t^2 = e^{\int_0^t \frac{g^2(\tau)}{\alpha_\tau^2} d\tau}$, $\bar{\alpha}_t = \frac{\alpha_t}{\alpha_1}$, and $\bar{\sigma} = \sigma_1^2 - \sigma_t^2$ are determined by \mathbf{f} and g . Therefore, the marginal distribution follows a Gaussian form, expressed as

$$p_t(X_t | X_0, X_1) = \mathcal{N}(\mu_x(X_0, X_1, t), \sigma_x^2(t)I), \quad (3)$$

where we have the mean $\mu_x(X_0, X_1, t) = (\alpha_t \bar{\sigma}_t^2 X_0 + \bar{\alpha}_t \bar{\sigma}_t^2 X_1) / \sigma_1^2$ and the variance $\sigma_x^2(t) = \alpha_t^2 \bar{\sigma}_t^2 \sigma_t^2 / \sigma_1^2$.

The training objective in inverse problems is to reconstruct clean data. Therefore, we perform the widely-adopt data prediction objective (Jukić et al. 2024) to optimize a neural network X_θ to predict X_0 given X_t as,

$$\min_{\theta} \mathbb{E}_{X_t \sim p_{t|0}} [\|X_\theta(X_t, t, X_1) - X\|_2^2], \quad (4)$$

where X_1 serves as a condition of the network.

During inference, the inverse problems can be solved by calling X_θ to compute the score $\nabla \log \hat{\Psi}_t$ iteratively. Specifically, given a SB state X_τ at time τ , the state X_t at $t \in [0, \tau)$ can be obtained by a first-order SDE sampler as,

$$X_t = W_\tau \frac{\alpha_t}{\alpha_\tau} X_\tau + W_0 \alpha_t X_\theta(X_\tau, \tau, X_1) + \alpha_t \sigma_t \sqrt{1 - \frac{\sigma_t^2}{\sigma_\tau^2}} \mathbf{z} \quad (5)$$

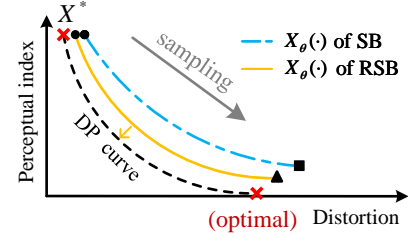


Figure 1: DP tradeoff. The smaller the values on both axes, the better the solution quality.

where $W_\tau = \sigma_t^2 / \sigma_\tau^2$, $W_0 = 1 - \sigma_t^2 / \sigma_\tau^2$, and $\mathbf{z} \sim \mathcal{N}(0, I)$. Similarly, the ordinary differential equation (ODE) formulation of Eq. (1) can be solved by the ODE sampler (Jukić et al. 2024). Finally, the final state $X_0 = X_\theta(X_\tau, \tau, X_1)$ at $t = 0$ (where $\sigma_0 = 0$) is the model prediction at the final sampling step and the solution \hat{X} of inverse problems (the bottom-right endpoint of the blue curve in Figure 1).

DP Tradeoff & Exposure Bias via Prediction Errors.

Next, we analyze the DP tradeoff and the exposure bias of the SB-based model in inverse problems from the perspective of prediction errors and motivate our RSB model.

Prediction Errors. We begin by recalling the training objective as Eq. (4) to observe the model predictions during inference. Specifically, at the initial step $t = 1$, the training objective collapses to a discriminative loss that prioritizes distortion minimization, so the prediction errors tend to the minimal MSE estimate (denoted as X^*) and the prediction of X is distortion-oriented. In contrast, at $t \rightarrow 0$, as the objective enforces p_{X_0} to approach the data distribution p_X , the model places greater emphasis on pushing predictions to match the distributional statistics of clean data given X_1 . In this case, the predictions resemble posterior samples and become perception-oriented rather than minimizing distortion for a particular y , resulting in the maximal prediction errors. For intermediate $t \in (0, 1)$, model predictions may evolve smoothly from distortion-oriented to perception-oriented estimates, forming a drift trajectory that interpolates between these two endpoints.

In summary, the SB training objective leads to prediction errors during inference, and the error drift exhibits the tradeoff between distortion and perception. Furthermore, input mismatch leads to error accumulation, resulting in an exposure bias problem. In order to address both issues, we need a novel training strategy that could regularize the prediction errors in inverse problems as detailed below.

DP Tradeoff. As for the DP tradeoff, in the inverse problem, the optimal tradeoff solution achieves optimal perception quality while minimizing the distortion. However, the vanilla SB is guided to reach the data distribution, pursuing high perception quality while sacrificing the distortion quality (i.e., reconstruction accuracy). As a result, the solution falls into the suboptimal case in inverse problems (illustrated as the blue dash-dot curve in Figure 1). As noted above, the

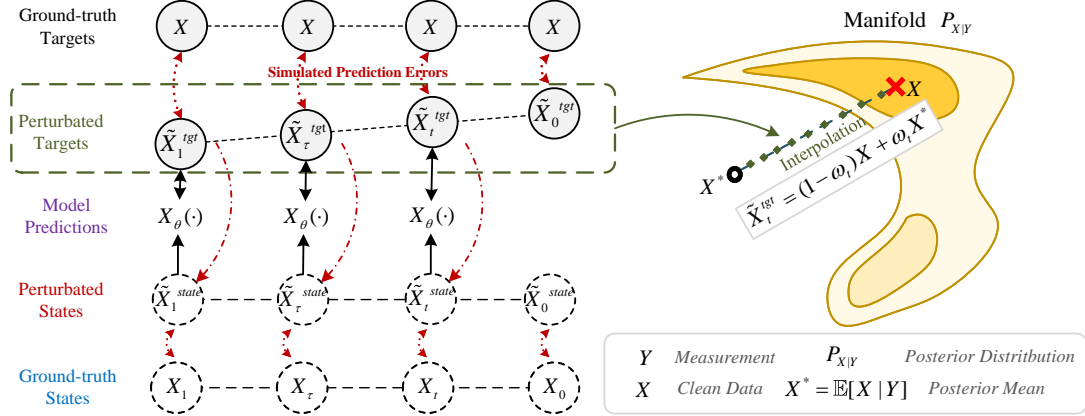


Figure 2: Schematic illustration of Distortion-Perception Regularization in our RSB, the key of which is the interpolation perturbation to both the training targets and input states.

prediction error drift reflects the DP tradeoff, encouraging our goal to design a new training target to guide the model predictions along the DP curve (the yellow curve in Figure 1), leading to the optimal solution of the DP tradeoff.

Exposure Bias. The input mismatch between training and inference, referred to as exposure bias, leads to the prediction errors accumulating along with the sampling trajectory, thereby degrading the final reconstruction quality in inverse problems. During training, the model is fed the real intermediate states, while at the inference stage, it receives the predicted states, but has never been exposed to its predictions. Thus, the vanilla SB objective is optimized under real states but does not account for the unseen inference-time input. So, the key to eliminating exposure bias is to align the inputs of the training-reference stages by estimating the prediction errors, and meanwhile, exposing the model training to the estimated inference-time errors.

Distortion-Perception Regularization

In this section, we propose a novel SB-based solution for inverse problems through DP regularization. Different from the previous regularization attempts in diffusion-based image synthesis (Ning et al. 2023b; Ren et al. 2024), which passively improve robustness by simply perturbing the model inputs with Gaussian noise, our DP regularization proposes an interpolation perturbation to actively guide the model predictions towards the optimal DP tradeoff, thereby transforming the training dynamics into a targeted pursuit of a theoretically superior solution.

Overall, as shown in Figure 2, DP regularization perturbs training targets through the interpolation between the distortion-optimal endpoint X^* (i.e., posterior mean) and the perception-optimal endpoint X . That is, the prediction errors can be defined as a time-varying distance between the two endpoints. This interpolation enables the model to traverse the DP tradeoff curve during training, that is, to approach the optimal tradeoff solution of inverse problems. Additionally, the model is exposed to the simulated prediction errors, mitigating the training-inference mismatch and

reducing exposure bias. Note that such perturbations smooth the training targets from distortion-optimal to perception-optimal estimates. Thus, it can be considered as a label smoothing regularization technique (Cheng et al. 2021), and we refer to it as DP regularization.

Perturbation Design. Recall that the model predictions show a patterned and time-varying drift, so we can design a perturbation on the real data X to match the prediction drift, thereby simulating the prediction errors. Since the theoretical optimal solutions on the DP curve take an interpolation form (Freirich, Michaeli, and Meir 2021), we construct our perturbation by forming an interpolation between the real data X (the perception-optimal endpoint) and the minimal MSE estimate X^* (the distortion-optimal endpoint) and define the new training targets \tilde{X}_t^{tgt} for the network X_θ ,

$$\tilde{X}_t^{tgt} = (1 - \omega_t)X + \omega_t X^*, \quad (6)$$

where ω_t is a time-varying weight, which has $\omega_0 = 0$ and $\omega_1 = 1$. As our goal is to obtain a better tradeoff that maintains high perception while achieving lower distortion, ω_t needs to grow slowly for smaller t , so that the training targets stay close to the ground-truth data X . For simplicity, we empirically set $\omega_t = t^2$. Additionally, we utilize an auxiliary predictive task to produce X^* . A predictive model D_ϕ is trained with the MSE training objective. After well training, the prediction of D_ϕ given Y is considered to approximate X^* with respect to X , namely $X^* \approx D_\phi(Y)$.

Note that prediction errors are simulated as $\omega_t(X^* - X)$. As shown in Figure 2, we introduce a larger simulated error at larger t to improve the robustness of the model to inevitable early-stage prediction errors. While at smaller t , the model is encouraged to progressively correct its outputs, gradually aligning them with the true data distribution.

Following Eq. (3), we can obtain the perturbed intermediate states with prediction errors as the model input,

$$\tilde{X}_t^{state} = \mu_x(\tilde{X}_t^{tgt}, X_1, t) + \sigma_x(t)\mathbf{z}, \quad \mathbf{z} \sim \mathcal{N}(0, \mathbf{I}). \quad (7)$$

Regularizing Training with Perturbation. To regularize model training, we adopt our perturbations into the training

Algorithm 1: Training procedure of RSB

Require: dataset $\mathcal{D} = \{(x, y)\}$, G_θ , pretrained D_ϕ
repeat
 Draw $(x, y) \sim \mathcal{D}$ and $t \sim \mathcal{U}([t_\epsilon, 1])$
 $x^* \leftarrow D_\phi(y)$
 Obtain perturbed targets \tilde{x}_t^{tgt} via Eq. (6)
 Sample perturbed states \tilde{x}_t^{state} from Eq. (7)
 Compute $X_\theta(\tilde{X}_t^{state}, t, y)$ and update θ using Eq. (8)
until converged

objective. Specifically, we replace the ground-truth training target X and the input state X_t in Eq. (4) with our perturbed counterparts, \tilde{X}_t^{tgt} (Eq. (6)) and \tilde{X}_t^{state} (Eq. (7)), respectively. Hence, our RSB can be formalized with the following regularized training objective,

$$\min_{\theta} \mathbb{E}_{\tilde{X}_t^{state}, t} [\|X_\theta(\tilde{X}_t^{state}, t, X_1) - \tilde{X}_t^{tgt}\|_2]. \quad (8)$$

Algorithm 1 details the training process, and RSB employs the same SDE sampler (Eq. (5)) as the vanilla SB.

When the regularized objective is optimized, our RSB is exposed to the simulated inference-time prediction errors, mitigating the training-inference mismatch and reducing exposure bias. Furthermore, by perturbing targets in our objective (Eq. (8)) and designing the interpolation perturbation to emulate the endpoints and tradeoff characteristics of the DP curve, RSB explicitly models the minimum distortion path across varying perceptual quality levels. This allows RSB to traverse the DP curve, approaching optimal perception quality with minimal distortion. As a result, RSB framework can produce more faithful and perceptually plausible reconstructions in ill-posed settings.

Experimental Evaluation

This section validates the effectiveness of RSB on two typical audio inverse tasks for speech enhancement: speech denoising and dereverberation.

Datasets

WSJ0+WHAM is a synthetic speech denoising dataset, utilizing clean utterances from WSJ0 dataset (Garofolo et al. 2007). The noise recordings are from WHAM noise corpus (Wichern et al. 2019). Each clean utterance is mixed with a randomly selected WHAM noise segment at a Signal-to-Noise Ratio (SNR) uniformly drawn from -6 dB to 14 dB. The training set uses the `si_tr_s` subset of WSJ0, containing 25550 mixtures (≈ 50 h), while the validation and test sets correspond to `si_et_05` and `si_dt_05`, containing 1302 and 2412 mixtures, respectively.

VoiceBank+DEMAND (Valentini Botinhao et al. 2016) is a widely-used speech denoising benchmark. Each clean utterance from VoiceBank (Veaux, Yamagishi, and King 2013) is mixed with one of ten noise recordings, including eight DEMAND recordings (Thiemann, Ito, and Vincent 2013) and two synthetic noises. Mixtures are generated at 15, 10, 5, and 0 dB SNR for training and at 17.5, 12.5, 7.5, and 2.5 dB SNR for testing.

Strategy	PESQ↑	CSIG↑	SBAK↑	COVL↑	SI-SDR↑
No	3.04	4.05	3.47	3.56	17.8
Input-only	2.98	4.02	3.44	3.50	18.1
Joint	3.04	4.08	3.51	3.57	18.8

Table 1: Speech denoising results on VoiceBank+DEMAND using different perturbation strategies.

WSJ0+Reverb is constructed for speech dereverberation with the same data split as WSJ0+WHAM. The degraded speech is generated by convolving the clean utterances from WSJ0 with synthetic room-impulse responses generated using the image-source method (Lemercier et al. 2023).

Evaluation Metrics

Distortion-oriented. These metrics quantify point-wise distortion between the enhanced signal and the clean reference. We report Scale-Invariant Signal-to-Distortion Ratio (SI-SDR) (Le Roux et al. 2019), Scale-Invariant Signal-to-Interference Ratio (SI-SIR), and Scale-Invariant Signal-to-Artifact Ratio (SI-SAR), which measure overall distortion, interference, and algorithmic artifacts, respectively.

Perception-oriented. These metrics measure overall perceptual quality. We include Perceptual Evaluation of Speech Quality (PESQ) (Rix et al. 2001), the composite metrics CSIG, CBAK, and COVL (Hu and Loizou 2008) (predicting the Mean Opinion Scores (MOS) for perceived signal fidelity, background intrusiveness, and overall quality, respectively), the non-intrusive DNSMOS P.808 metric (Reddy, Gopal, and Cutler 2021) for reference-free estimation, and Extended Short-Time Objective Intelligibility (ESTOI) (Jensen and Taal 2016) for intelligibility.

Implementation Details

For noise schedule, we use the Variance Exploding setting recommended in (Jukić et al. 2024) for both SB and RSB, which have $f(t) = 0$, $g^2(t) = ck^{2t}$, $\alpha_t = 1$ and $\sigma_t^2 = \frac{c(k^{2t}-1)}{2\log k}$, where $c = 0.40$ and $k = 2.6$. We implement X_θ and predictive model D_θ based on NCSN++M (Richter et al. 2023), which has approximately 25.2 M parameters. All audio recordings are resampled to 16 kHz, and the complex spectrogram features are extracted with the same setting as (Lemercier et al. 2023). All models are trained on one NVIDIA A100 GPU. The batch size is set to 16, and the optimizer is Adam (Kingma and Ba 2015) with a learning rate of 10^{-4} . The minimal time t_ϵ during training is set to 10^{-4} . We compute the loss in Eq. (8) on the complex spectrogram, and introduce an additional time-domain reconstruction loss following Jukić et al.. We train our models in all experiments for 1000 epochs and employ an early stopping strategy based on the SI-SDR value of 50 validation samples, with a patience of 20 (Lemercier et al. 2023). For stable training and generalization, we maintain an Exponential Moving Average (EMA) version of the model parameters with a decay of 0.999 during training. The best EMA checkpoint is selected based on the PESQ value (Lemercier

Method	PESQ \uparrow	CSIG \uparrow	CBAK \uparrow	COVL \uparrow	DNSMOS \uparrow	SI-SDR \uparrow	SI-SIR \uparrow	SI-SAR \uparrow
unprocessed	1.32 \pm 0.30	2.78 \pm 0.67	1.91 \pm 0.50	1.99 \pm 0.49	2.71 \pm 0.30	3.9 \pm 5.8	3.9 \pm 5.8	—
NCSN++M	2.18 \pm 0.62	3.05 \pm 0.80	2.97 \pm 0.56	2.58 \pm 0.74	3.77 \pm 0.35	14.7 \pm 4.2	29.5 \pm 4.4	14.9 \pm 4.3
SB	2.54 \pm 0.62	3.93 \pm 0.62	3.12 \pm 0.53	3.22 \pm 0.62	3.74 \pm 0.39	13.2 \pm 4.3	29.2 \pm 4.6	13.4 \pm 4.4
RSB (ours)	2.61 \pm 0.60	4.00 \pm 0.59	3.18 \pm 0.51	3.30 \pm 0.60	3.73 \pm 0.39	13.7 \pm 4.1	29.5 \pm 4.6	13.8 \pm 4.2

Table 2: Speech denoising results on WSJ0+WHAM. All values are reported as mean and standard deviation.

Method	PESQ \uparrow	CSIG \uparrow	CBAK \uparrow	COVL \uparrow	DNSMOS \uparrow	SI-SDR \uparrow	SI-SIR \uparrow	SI-SAR \uparrow
unprocessed	1.38 \pm 0.26	2.93 \pm 0.41	1.72 \pm 0.28	2.09 \pm 0.35	2.88 \pm 0.27	-9.1 \pm 6.6	-9.1 \pm 6.6	—
NCSN++M	1.96 \pm 0.47	3.29 \pm 0.53	2.55 \pm 0.39	2.59 \pm 0.51	3.52 \pm 0.37	4.8 \pm 4.4	23.6 \pm 9.5	5.0 \pm 4.4
SB	2.58 \pm 0.49	4.18 \pm 0.39	2.92 \pm 0.37	3.38 \pm 0.45	3.71 \pm 0.39	4.6 \pm 4.7	25.1 \pm 10.4	4.7 \pm 4.4
RSB (ours)	2.59 \pm 0.49	4.18 \pm 0.39	2.94 \pm 0.38	3.38 \pm 0.45	3.71 \pm 0.39	5.2 \pm 4.5	26.0 \pm 10.1	5.3 \pm 4.3

Table 3: Speech dereverberation results on WSJ0+Reverb. All values are reported as mean and standard deviation.

Method	PESQ \uparrow	ESTOI \uparrow	DNSMOS \uparrow	SI-SDR \uparrow
unprocessed	1.97	0.79	3.02	8.4
NCSN++M	2.86	0.87	3.59	19.9
CDiffuse	2.52	0.79	3.08	12.4
SGMSE+	2.81	0.86	3.55	17.5
StoRM	2.88	0.87	3.53	18.5
SB	3.04	0.87	3.57	17.8
RSB (ours)	3.04	0.87	3.56	18.8

Table 4: Denoising performance comparison with baselines on VoiceBank+DEMAND.

et al. 2023). We initially train the predictive model D_ϕ and then train X_θ with the parameter ϕ frozen. SB and RSB use the same SDE sampler described in Eq. (5). The source code, included in the supplementary materials, will be made publicly available upon acceptance.

Ablation study

Table 1 summarizes the effects of input and target perturbations during training. **No perturbation** corresponds to the vanilla SB setup and serves as the baseline. **Input-only perturbation** improves SI-SDR by only 0.3 dB but slightly degrades the MOS-derived metrics, suggesting that perturbing the input alone may introduce additional errors. In contrast, **joint input-target perturbation** achieves the best trade-off: SI-SDR increases to 18.8 dB, while PESQ reaches its highest value, and CSIG, SBAK, and COVL are further improved. These gains in composite metrics indicate better preservation of the clean signal, greater noise suppression, and enhanced overall perception quality. Joint perturbation enables model training to recover from input perturbation-induced errors and guides predictions onto the DP curve. Therefore, RSB adopts a joint perturbation strategy as the foundation of our DP regularization.

Performance Comparison

We compare RSB against purely predictive backbone NCSN++M (Richter et al. 2023) and diffusion-based gen-

erative SE methods including CDiffuse (Lu et al. 2022), SGMSE+ (Richter et al. 2023), StoRM (Lemercier et al. 2023) and SB (Jukić et al. 2024). Unless specified, all methods use 50 sampling steps for inference, except for the 6-step setting of CDiffuse (Lu et al. 2022). It is worth noting that SGMSE+ and StoRM employ a predictor-corrector sampler, which means a total of 100 network calls (Richter et al. 2023; Lemercier et al. 2023). SGMSE+, StoRM, SB, and RSB share the same network architecture.

Results on WSJ0+WHAM and WSJ0+Reverb We first compare the denoising performance of RSB with baselines on the WSJ0+WHAM dataset. As shown in Table 2, RSB obtains the best perceptual scores across all MOS-derived metrics, surpassing both the predictive baseline NCSN++M and vanilla SB. Although NCSN++M maintains a slight advantage in DNSMOS and achieves the highest SI-SDR, this comes at the cost of significantly worse perceptual quality (e.g., 0.43 score lower PESQ than RSB). Notably, compared with SB, RSB further narrows the distortion gap to NCSN++M while improving every perceptual metric, indicating that our regularization balances perceptual quality and distortion more effectively. The improvement of SI-SIR and SI-SAR further confirms that the superior performance of RSB is not achieved by introducing spurious artifacts or excessive residual noise.

Table 3 presents the dereverberation performance on the WSJ0+Reverb dataset. RSB matches or exceeds the best scores in all perception-oriented metrics, and outperforms all baselines in all distortion-oriented metrics. It further demonstrates its superiority in both perceptual and distortion metrics. These results confirm that RSB steers the solution closer to the optimal DP tradeoff.

Results on VoiceBank+DEMAND Table 4 shows the denoising performance on the VoiceBank+DEMAND benchmark. RSB achieves the highest SI-SDR and matches SB in PESQ and ESTOI. The performance gap between SB and RSB is smaller than on WSJ0+WHAM because VoiceBank+DEMAND uses only positive SNRs around 10 dB and simpler noise conditions. RSB still improves SI-SDR by 1.0 dB over SB while maintaining top perceptual scores. This

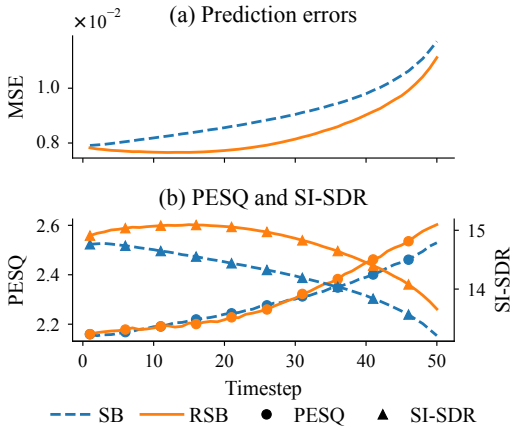


Figure 3: Prediction errors (a) and evaluation metrics (b) during 50-step sampling on WSJ0+WHAM. The prediction errors at each timestep are calculated as $\mathbb{E}[\|X_\theta(\cdot) - X\|_2^2]$.

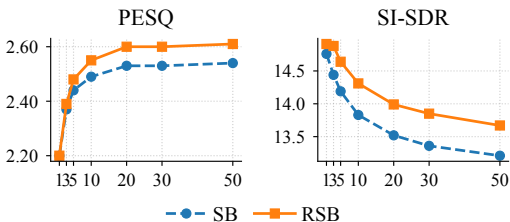


Figure 4: Speech denoising performance on WSJ0+WHAM as a function of the number of sampling steps.

result indicates that DP regularization can improve performance across various SNR settings.

Effectiveness in Mitigating Exposure Bias

Figure 3 (a) plots the per-step prediction error over 50 sampling steps on WSJ0+WHAM to evaluate exposure bias. The error trajectory of vanilla SB exhibits an accelerating error growth as sampling progresses, underscoring the need to mitigate exposure bias and enhance robustness to its own predictions. In contrast, RSB yields a markedly flatter curve in early steps, indicating slower error accumulation. Additionally, empirically validating our observation, the increased prediction error in later sampling steps arises as the model prioritizes alignment with the data distribution over reconstruction accuracy. Consequently, RSB achieves lower final prediction errors, delivering higher reconstruction accuracy. In Figure 3 (b), PESQ and SI-SDR are chosen to quantify the perception and distortion quality of model predictions. RSB achieves better PESQ (perceptual quality) and SI-SDR (distortion quality) scores than SB. This confirms that RSB not only mitigates exposure bias more effectively but also produces higher-quality solutions.

Evaluating the Distortion–Perception Tradeoff

Number of sampling steps vs. DP tradeoff Figure 4 analyzes the DP tradeoff of SB and RSB under varying sampling steps on WSJ0+WHAM. PESQ rises sharply in early

Method	PESQ↑	CSIG↑	SBAK↑	COVL↑	SI-SDR↑
M1	3.04	4.05	3.47	3.56	17.8
M2	3.02	4.05	3.45	3.54	18.0
M3	2.96	4.03	3.40	3.50	17.7
M4	2.95	4.01	3.40	3.48	17.8
M5	3.04	4.08	3.51	3.57	18.8

Table 5: Speech denoising results on VoiceBank+DEMAND using different DP tradeoff strategies.

steps and quickly saturates, indicating fast convergence in perceptual quality, while SI-SDR gradually decreases as perceptual quality increases, reflecting the DP tradeoff. Notably, RSB consistently achieves higher PESQ and better preserves SI-SDR across all steps, with a significantly slower degradation. This demonstrates that while perceptual quality improves at the expense of reconstruction accuracy, RSB attains high perceptual quality earlier while maintaining distortion performance, thereby achieving a more favorable DP trade-off than SB.

Tradeoff strategies vs. DP tradeoff Table 5 compares different strategies for improving the DP tradeoff on VoiceBank+DEMAND. The vanilla SB (M1) achieves strong perceptual quality and serves as the baseline for other variants (M2–M5). M2 uses the minimal MSE estimate as the starting point of SB sampling, improving distortion performance. M3 utilizes the minimal MSE estimate as the conditioning of SB, where M4 considers it both as the starting point and conditioning. The result shows that M3 and M4 underperform M1 in both distortion and perception quality. This indicates that the minimal MSE estimate may overly constrain the SB and limit exploration of perceptually favorable solutions, leading to suboptimal tradeoffs. In contrast, our RSB (M5) gets the best overall DP balance, achieving superior distortion reduction and maintaining perceptual quality. Significantly, while M2–M4 require the predictive model to generate the minimal MSE estimates on the fly during inference, RSB only relies on the predictive model during training and eliminates this dependency at inference time. Finally, based on the advanced DP Regularization strategy, our RSB thus offers a simple yet effective framework that achieves a more favorable DP tradeoff of the inverse problem.

Conclusion

RSB aims to address two challenges of SB in solving inverse problems: the DP tradeoff and exposure bias. It introduces an advanced training regularization to simulate prediction errors, mitigating the training–inference mismatch and thus reducing the exposure bias, and encourages model predictions to approach the DP curve, achieving a better tradeoff and thus alleviating distortion. In the SE task, RSB outperforms state-of-the-art generative methods, especially with respect to distortion-oriented metrics and exposure bias reduction. Furthermore, RSB is readily applicable to a wide range of inverse problems beyond speech enhancement, such as image denoising, deblurring, and inpainting.

References

Adrai, T.; Ohayon, G.; Michaeli, T.; and Elad, M. 2023. Deep Optimal Transport: A Practical Algorithm for Photo-realistic Image Restoration. In *Advances in Neural Information Processing Systems*, 61777–61791.

Blau, Y.; and Michaeli, T. 2017. The Perception-Distortion Tradeoff. In *Proceedings of the IEEE/CVF Conference on Computer Vision and Pattern Recognition*, 6228–6237.

Chen, T. Q.; Liu, G.-H.; and Theodorou, E. A. 2022. Likelihood Training of Schrödinger Bridge using Forward-Backward SDEs Theory. In *International Conference on Learning Representations*.

Chen, Z.; He, G.; Zheng, K.; Tan, X.; and Zhu, J. 2023. Schrödinger Bridges Beat Diffusion Models on Text-to-Speech Synthesis. arXiv:2312.03491.

Cheng, M.; Chen, P.-Y.; Liu, S.; Chang, S.; Hsieh, C.-J.; and Das, P. 2021. Self-progressing robust training. In *Proceedings of the AAAI Conference on Artificial Intelligence*, volume 35, 7107–7115.

Freirich, D.; Michaeli, T.; and Meir, R. 2021. A Theory of the Distortion-Perception Tradeoff in Wasserstein Space. In *Advances in Neural Information Processing Systems*.

Garofolo, J. S.; Graff, D.; Paul, D.; and Pallett, D. 2007. CSR-I (WSJ0) Complete. <https://catalog.ldc.upenn.edu/LDC93S6A>.

Ho, J.; Jain, A.; and Abbeel, P. 2020. Denoising Diffusion Probabilistic Models. In *Advances in Neural Information Processing Systems*, 6840–6851.

Hu, Y.; and Loizou, P. C. 2008. Evaluation of Objective Quality Measures for Speech Enhancement. *IEEE Transactions on Audio, Speech and Language Processing*, 16(1): 229–238.

Jensen, J.; and Taal, C. H. 2016. An Algorithm for Predicting the Intelligibility of Speech Masked by Modulated Noise Maskers. *IEEE Transactions on Audio, Speech and Language Processing*, 24(11): 2009–2022.

Jukić, A.; Korostik, R.; Balam, J.; and Ginsburg, B. 2024. Schrödinger Bridge for Generative Speech Enhancement. In *Proceedings of Interspeech*.

Kantorovich, L. V. 2006. On the Translocation of Masses. *Journal of Mathematical Sciences*, 133(4): 1381–1382.

Kawar, B.; Elad, M.; Ermon, S.; and Song, J. 2022. Denoising Diffusion Restoration Models. In *Advances in Neural Information Processing Systems*.

Kingma, D. P.; and Ba, J. 2015. Adam: A Method for Stochastic Optimization. In *International Conference on Learning Representations*.

Le Roux, J.; Wisdom, S.; Erdogan, H.; and Hershey, J. R. 2019. SDR – Half-baked or Well Done? In *Proceedings of the IEEE International Conference on Acoustics, Speech and Signal Processing*, 626–630.

Lemercier, J.-M.; Richter, J.; Welker, S.; and Gerkmann, T. 2023. StoRM: A Diffusion-Based Stochastic Regeneration Model for Speech Enhancement and Dereverberation. *IEEE Transactions on Audio, Speech and Language Processing*, 31: 2724–2737.

Li, M.; Qu, T.; Sun, W.; and Moens, M.-F. 2023. Alleviating Exposure Bias in Diffusion Models through Sampling with Shifted Time Steps. In *International Conference on Learning Representations*.

Liu, G.-H.; Vahdat, A.; Huang, D.-A.; Theodorou, E. A.; Nie, W.; and Anandkumar, A. 2023. I2SB: Image-to-Image Schrödinger Bridge. In *International Conference on Machine Learning*, volume 202, 22042–22062.

Lu, Y.-J.; Wang, Z.-Q.; Watanabe, S.; Richard, A.; Yu, C.; and Tsao, Y. 2022. Conditional Diffusion Probabilistic Model for Speech Enhancement. In *Proceedings of the IEEE International Conference on Acoustics, Speech and Signal Processing*, 7402–7406.

Ning, M.; Li, M.; Su, J.; Salah, A. A.; and Ertugrul, I. O. 2023a. Elucidating the Exposure Bias in Diffusion Models. In *International Conference on Learning Representations*.

Ning, M.; Sangineto, E.; Porrello, A.; Calderara, S.; and Cucchiara, R. 2023b. Input Perturbation Reduces Exposure Bias in Diffusion Models. In *International Conference on Machine Learning*, 26245–26265.

Ohayon, G.; Michaeli, T.; and Elad, M. 2025. Posterior-Mean Rectified Flow: Towards Minimum MSE Photo-Realistic Image Restoration. In *The Thirteenth International Conference on Learning Representations*.

Ongie, G.; Jalal, A.; Metzler, C. A.; Baraniuk, R.; Dimakis, A. G.; and Willett, R. M. 2020. Deep Learning Techniques for Inverse Problems in Imaging. *IEEE Journal on Selected Areas in Information Theory*, 1: 39–56.

Reddy, C. K.; Gopal, V.; and Cutler, R. 2021. DNSMOS: A Non-Intrusive Perceptual Objective Speech Quality Metric to Evaluate Noise Suppressors. In *Proceedings of the IEEE International Conference on Acoustics, Speech and Signal Processing*, 6493–6497.

Ren, Z.; Zhan, Y.; Ding, L.; Wang, G.; Wang, C.; Fan, Z.; and Tao, D. 2024. Multi-Step Denoising Scheduled Sampling: Towards Alleviating Exposure Bias for Diffusion Models. In *Proceedings of the AAAI Conference on Artificial Intelligence*.

Richardson, W. H. 1972. Bayesian-Based Iterative Method of Image Restoration. *Journal of the Optical Society of America*, 62: 55–59.

Richter, J.; Welker, S.; Lemercier, J.-M.; Lay, B.; and Gerkmann, T. 2023. Speech Enhancement and Dereverberation with Diffusion-Based Generative Models. *IEEE Transactions on Audio, Speech and Language Processing*, 31: 2351–2364.

Rix, A. W.; Beerends, J. G.; Hollier, M. P.; and Hekstra, A. P. 2001. Perceptual Evaluation of Speech Quality (PESQ)-A New Method for Speech Quality Assessment of Telephone Networks and Codecs. In *Proceedings of the IEEE International Conference on Acoustics, Speech and Signal Processing*, 749–752.

Saharia, C.; Chan, W.; Chang, H.; Lee, C. A.; Ho, J.; Salimans, T.; Fleet, D. J.; and Norouzi, M. 2021. Palette: Image-to-Image Diffusion Models. *ACM SIGGRAPH 2022 Conference Proceedings*.

Song, Y.; Sohl-Dickstein, J.; Kingma, D. P.; Kumar, A.; Ermon, S.; and Poole, B. 2021. Score-Based Generative Modeling through Stochastic Differential Equations. In *International Conference on Learning Representations*.

Thiemann, J.; Ito, N.; and Vincent, E. 2013. The Diverse Environments Multi-Channel Acoustic Noise Database: A Database of Multichannel Environmental Noise Recordings. *The Journal of the Acoustical Society of America*, 133(5).

Valentini Botinhao, C.; Wang, X.; Takaki, S.; and Yamagishi, J. 2016. Investigating RNN-Based Speech Enhancement Methods for Noise-Robust Text-to-Speech. In *Proceedings of ISCA Speech Synthesis Workshop*, 146–152.

Veaux, C.; Yamagishi, J.; and King, S. 2013. The Voice Bank Corpus: Design, Collection and Data Analysis of A Large Regional Accent Speech Database. In *OCOCOSDA/CASLRE*.

Wang, P.; Xiao, B.; He, Q.; Glide-Hurst, C. K.; and Dong, M. 2024. Score-Based Image-to-Image Brownian Bridge. *Proceedings of the ACM International Conference on Multimedia*, 2024: 10765 – 10773.

Whang, J.; Delbracio, M.; Talebi, H.; Saharia, C.; Dimakis, A. G.; and Milanfar, P. 2021. Deblurring via Stochastic Refinement. In *Proceedings of the IEEE/CVF Conference on Computer Vision and Pattern Recognition*, 16272–16282.

Wichern, G.; Antognini, J.; Flynn, M.; Zhu, L. R.; McQuinn, E.; Crow, D.; Manilow, E.; and Le Roux, J. 2019. WHAM!: Extending Speech Separation to Noisy Environments. In *Proceedings of Interspeech*, 1368–1372.

Zhou, C.; Lu, G.; Li, J.; Chen, X.; Cheng, Z.; Song, L.; and Zhang, W. 2025. Controllable Distortion-Perception Trade-off Through Latent Diffusion for Neural Image Compression. In *Proceedings of the AAAI Conference on Artificial Intelligence*.

Zhou, L.; Lou, A.; Khanna, S.; and Ermon, S. 2023. Denoising Diffusion Bridge Models. In *International Conference on Learning Representations*.